Hybridized quadrupole-dipole exciton effects in a Cu_2O-organic heterostructure

Oleksiy Roslyak and Joseph L. Birman
Physics Department, The City College, CUNY, Convent Avenue at 138 Street, New York, New York 10031, USA
(Received 2 January 2007; revised manuscript received 10 March 2007; published 6 June 2007)

In the present work, we discuss resonant hybridization of the 1*S* quadrupole Wannier-Mott exciton (WE) in a Cu_2O quantum well with the Frenkel dipole exciton in an adjacent layer of organic DCM2:CA:PA. The coupling between excitons is due to interaction between the gradient of electric field induced by the DCM2 Frenkel exciton (FE) and the quadrupole moment of the 1*S* transition in the cuprous oxide. The specific choice of the organic allows us to use the mechanism of "solid state solvation" [C. Madigan and V. Bulovic, Phys. Rev. Lett. **91**, 247403 (2003)] to dynamically tune the WE and FE into resonance for ≈3.3 ns (comparable with the big lifetime of the WE) of the "slow" phase of the solvation. The quadrupole-dipole hybrid utilizes the big oscillator strength of the FE, along with the big lifetime of the quadrupole exciton, unlike dipole-dipole hybrid exciton which utilizes the big oscillator strength of the FE and big radius of the dipole allowed WE. Due to the strong spatial dispersion and big mass of the quadrupole WE, the hybridization is not masked by the kinetic energy or the radiative broadening. The lower branch of the hybrid dispersion exhibits a pronounced minimum and may be used in applications. Also, we investigate and report noticeable change in the coupling due to an induced "Stark effect" from the strong local electric field of the FE. We investigated the fine energy structure of the quantum well confined ortho and para excitons in cuprous oxide.

DOI: 10.1103/PhysRevB.75.245309 PACS number(s): 71.35.Cc, 79.60.Jv

I. INTRODUCTION

Nanometer-sized organic and inorganic semiconductor structures have recently been attracting much attention. In these low-dimensional systems, there are pronounced quantum confinement effects on the electronic and optical properties. Synthesizing composite organic-inorganic semiconductors is of major importance not only in the development of novel nanostructure materials for electronics, optics, and transport, but also for basic understanding of their size-dependent physical properties. Recently, a new type of elementary state which can be generated by optical excitation was discussed by Agranovich *et al.*[1] This is a hybrid exciton which can be obtained from the resonant mixing of Frenkel exciton (FE) and Wannier-Mott exciton (WE) in organic-inorganic quantum wells by means of dipole-dipole interaction across the interface. Many properties of this hybrid were predicted. Other realizations for the hybrid have been proposed. Examples are hybrid excitons in an inorganic semiconducting quantum dot covered by an organic layer[2] and quantum dot–dendrimer system.[3] The energy of the hybrid exciton, as well as the Green's function matrix elements for different quantum dot–dendrimer systems, has been calculated.

In the model of Agranovich *et al.*, the decisive role in implementing the formation of the hybrid state is played by the dipole-dipole coupling between semiconductor WE and organic FE. It is assumed that there is no direct wave function overlap between the excitons on each side of the well. The interaction energy takes the form $P(\mathbf{r})\cdot E(\mathbf{r})$, where $P(\mathbf{r})$ is the polarization field due to the organic dipoles of the FE interacting with the electric field $E(\mathbf{r})$ in the semiconductor from WE. In the work reported here, we modified this model to consider the quadrupole exciton "yellow" 1*S* level in Cu_2O, which is well known from many studies on bulk Cu_2O. This immediately puts our attention on a different interaction term, which is now $Q_{i,j}\frac{\partial}{\partial_i}E_{j,\mathbf{k}}$. Here, the quadrupole field couples to a spatially varying (or k dependent) electric field. This coupling is the basis of the present work.[4] In this paper, we examine the new hybrid exciton which occurs in a Cu_2O-organic heterostructure. Although the oscillator strength of the quadrupole transition is 3 orders of magnitude smaller than that of the corresponding dipole case, we show here how this can be compensated by the strong spatial dispersion of the transition.

In Sec. II, generalizing the work[5] on dipole-dipole hybrid excitons, formed in adjacent layers of organic-inorganic heterostructures, we will introduce here a modification. The system we will analyze in this paper makes use of dipole forbidden, quadrupole 1*S* exciton in Cu_2O (WE) coupled to a suitable organic FE. From the fact of strong spatial dispersion of the quadrupole transitions, we anticipate strong wave vector and polarization dependence of the dispersion for the hybrid. Concrete results will be given below for a realistic configuration and values of parameters for particular organic materials.

To the best of our knowledge, there are no experimental studies yet on confinement effects for the cuprous oxide exciton in a quantum well. Therefore, in Sec. III, we present theoretical examination of confinement effects which are essential due to the rather small Bohr radius of 1*S* exciton, and central cell and field effects on the exciton dispersion.

In Sec. IV, we discuss the choice of some proper organic materials to assure resonance between FE and WE in the quantum wells. We are going to show that layers of polystyrene (PS): camorphic anhydride CCA):[2-methyl-6-2C2,3,6,7-tetrahydro-2*H*,5*H*-benzo[*i*,*j*]-quinolizin-a-yl)-ethyl]-4*H*-pyran-4-ylidene] propanel dinitrile CDCM2 (Ref. 6) give an excellent match to the quadrupole yellow exciton of Cu_2O. We have chosen this organic compound due to three main factors:

(1) the extremely big oscillator strength of the organic Frenkel exciton formed on DCM2 molecules;

(2) unlike the conventional organic with short emission lifetime, the dynamic "solid state solvation" mechanism discovered in such a compound would allow the hybrid to live through the phase of "slow" solvation (≈3 ns), which is comparable to the lifetime of the quadrupole exciton;

(3) the ability to tune into resonance the energy of the singlet FE simply by means of changing the concentration of the CA.

The strong local electric field induced by the organic Frenkel excitons penetrates into the cuprous oxide layer and results in an induced "confined Stark effect." Relative shift of the electron and hole gives rise to induced polarization and reduced hybridization effect. This will be discussed in detail in Sec. V.

Hybridization requires coupling between the two excitons, and we will estimate the coupling coefficient in Sec. VI. The coupling between FE and WE in the case of quadrupole active 1*S* WE is due to the gradient of the field induced by the FE in the DCM2 organic. In the dipole-dipole hybrid exciton, one utilizes the big oscillator strength of the FE and big Bohr radius of the WE; in the case of quadrupole-dipole exciton, one utilizes the big oscillator strength of the FE and long lifetime of the WE, along with the enhanced spatial dispersion of the coupling parameter.

In Sec. VII, we will discuss the specifics of the quadrupole-dipole hybridization dispersion and briefly propose possible applications of such a hybridization. We look forward to experimental tests of our results, by means of new types of high precision spectroscopy which were invented recently.[7]

II. THE QUADRUPOLE-DIPOLE HYBRID EXCITON CONFIGURATION

Our proposed configuration of an experiment for obtaining the hybrid exciton is shown in the following diagram (see Fig. 1). In this simplified model, a monolayer of width $L_w \approx$ size of a unit cell of a 4.6 Å quantum well of Cu_2O [gap energy $E_g = 2.17$ eV (Ref. 7)] is placed on a thin film of the PS:CA:DCM2 organic (with the gap energy much bigger than that of the cuprous oxide). Obliquely incident (to assure x component of the exciton wave vector) photons of close energies excite the Wannier-Mott exciton in the cuprous oxide in resonance with the Frenkel exciton in DCM2. We consider DCM2 exciton as a two-dimensional (2D) lattice of dipoles $d_x = 12$ D at discrete sites **n**, placed at $z' \approx L_w/2$.

We treat the interaction of cuprous oxide quadrupole excitations only with DCM2 organic molecules in the quadruple approximation, since at the pumping laser frequency, only dipole forbidden transitions are allowed. Due to the small concentration of the DCM2 molecules, there is a "buffer" of PS between Cu_2O and DCM2 so that one may neglect the exciton wave function overlap and assume perfect 2D invariance of the system in the direction transverse to growth. Further on, we neglect the kinetic energy of the Wannier exciton. Indeed, as will be shown in detail in the next section, due to fluctuations of the inorganic quantum well (IQW) width, strong confinement of the exciton occurs,[8] compared to the kinetic energy for small wave vectors which

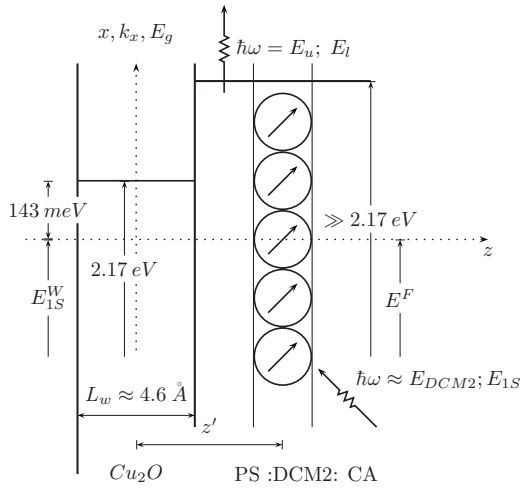

FIG. 1. Schematic representation of a possible experimental setup to produce quadrupole-dipole excitons. Here, the inorganic Cu_2O quantum well provides the Wannier-Mott 1*S* quadrupole exciton with the binding energy of 143 meV (for details, see Sec. III). Two pumping photons $\hbar\omega \approx E_{DCM2}, E_{1S}$ generate the hybrid signal from the upper E_u and lower E_l branches. The DCM2 part of the organic "solid state solute" provides the dipole allowed Frenkel exciton; the PS host prevents wave function overlapping between organic and inorganic excitons; CA under proper concentration allows tuning of the excitons into resonance. Due to the comparable lifetimes of both types of exciton, the system utilizes the strong spatial dispersion of the quadrupole exciton and big oscillator strength of the organic.

results in hopping motion of the exciton between sites of localization. We seek the new quadrupole-dipole hybrid eigenstates for the upper (u) and lower (l) branches in the usual linear combination form:

$$|u,\mathbf{k}\rangle = A_u|F,\mathbf{k}\rangle + B_u|W,\mathbf{k}\rangle, \quad |l,\mathbf{k}\rangle = A_l|F,\mathbf{k}\rangle + B_l|W,\mathbf{k}\rangle,$$

where the weighting coefficients for small **k** are given by[2] $A_{u,l}^2 = B_{u,l}^2 = 1/2$.

After the usual diagonalization of the coupled WE-FE Hamiltonian, $H = H_{WE} + H_{FE} + H_{int}$, the energies of the resulting upper and lower branches are given by

$$E_{u,l} = E^{W(F)} \pm \Gamma_{\mathbf{k}}$$

where we have introduced the quadrupole-dipole interaction Hamiltonian and corresponding off-diagonal hybridization parameter: $\Gamma(\mathbf{k}) \equiv |\langle W,\mathbf{k}|\hat{H}_{int}|F,\mathbf{k}\rangle|$.

In the subsequent sections, we will derive expressions for the energies of the exciton and necessary conditions for the resonance hybridization. Also, as a main result of the article, we will derive an analytical expression for the hybridization parameter and dispersion. This will be followed by quantitative and qualitative comparison of systems with dipole-dipole hybridization.[1]

III. QUASI-2D EXCITON IN Cu_2O

As far as we are aware, there are no experimental data or theoretical description for the film cuprous oxide systems,

TABLE I. Selection rules for the excitons in bulk Cu_2O. F, forbidden transition; A, allowed transition.

		O_h			
		Electric dipole operator	Electric quadrupole operator		
Symmetry		$^3\Gamma_4^-$	$^3\Gamma_5^+$	$^2\Gamma_3^+$	Basis
Para exciton	$^3\Gamma_2^+$	F	F	F	$(x^2-y^2)(y^2-z^2)(z^2-x^2)$
Ortho exciton	$^3\Gamma_5^+$	F	A	F	$xy;yz;zx$
Basis		$x;y;z$	$xy;yz;zx$	$2z^2-x^2-y^2$; $\sqrt{3}(x^2-y^2)$	

contrary to the extensive literature for the bulk case. In the case of the small size Cu_2O quadrupole exciton, one cannot consider strong confinement effect, which requires the width of the IQW to be much less than the Bohr radius of the exciton a_B. Even if modern epitaxy methods allows one to get a molecular monolayer for the quantum well thickness, one would have $L_w/a_B \approx 2/2$ which is not enough for pure 2D consideration. Two and more monolayers in one quantum well will give the case of weak confinement and result in much weaker coupling (see below). Thus, we start from the well described case of bulk yellow excitons and then estimate the main properties in the case of strong confinement theoretically.

Cu_2O condenses in a cubic structure, where the copper ions form a face-centered sublattice, while the oxygen ions form a body-centered sublattice. The arrangement of both sub lattices is such that a copper ion is found centered between two neighboring oxygen ions (O_h symmetry) with the lattice constant $a \approx 4.26$ Å. From the lattice structure, we now turn to the band structure of this crystal.[9] There is a direct band gap where the valence band is formed by the Cu $3d$ orbitals and the conduction band arises from Cu $4s$ and (possible) oxygen orbitals. When considering the cubic crystal field, the five $3d$ states of the valence band split further into three states of the $^3\Gamma_5^+$ type and a twofold $^2\Gamma_3^+$ level. Taking also spin-orbit interaction into account, the state splits further into a twofold $^2\Gamma_7^+$ level and a fourfold degenerate $^4\Gamma_8^+$ level. The exciton representation is obtained from the direct product of electron and hole, $\Gamma_{ex}=\Gamma_{envelop}\otimes\Gamma_e \otimes\Gamma_h$. For S excitons, $^1\Gamma_1^+\otimes{}^2\Gamma_7^+\otimes\Gamma_6^+={}^3\Gamma_5^+ + {}^1\Gamma_2^+$. The threefold degenerate $^3\Gamma_5^+$ state and single $^1\Gamma_2^+$ state are termed ortho exciton and para exciton, respectively. The para exciton is optically forbidden in bulk. The ortho exciton is dipole ($^3\Gamma_4^-$) forbidden from the ground state of symmetry ($^1\Gamma_1^+$), because $\langle {}^1\Gamma_1^+|{}^3\Gamma_4^-|{}^3\Gamma_5^+\rangle=0$ and couples to the light in lowest order via quadrupole interaction of symmetry ($^3\Gamma_5^+$), $\langle {}^1\Gamma_1^+|{}^3\Gamma_5^+|{}^3\Gamma_5^+\rangle \neq 0$.

Unlike the dipole operator, the quadrupole operator depends on the direction of the light wave vector $\mathbf{k}$ relative to the lattice and the radiation polarization vector $\mathbf{e}$. Because of the $\mathbf{k}$ dependence, the transition is anisotropic even in a cubic crystal. The amplitudes of the ortho-exciton quadrupole transitions are given by the symmetric vector product of $\mathbf{k}$ and $\mathbf{e}$: $\sim \mathbf{e}_i\mathbf{k}_j+\mathbf{e}_j\mathbf{k}_i$, $i \neq j$, see, for example, Ref. 9. The three components correspond to the Cartesian representations: $^3\Gamma_{5xz}^+$, $^3\Gamma_{5yz}^+$, $^3\Gamma_{5xy}^+$.

The measured[10] oscillator strength of the quadrupole transition in bulk Cu_2O is low, $f \simeq 3.9\times10^{-9}$, which is about 4 orders of magnitude smaller than the value found for the dipole transitions of the P excitons of the yellow series. Even though the coupling to the light is extremely weak, it cannot be disregarded. The binding energy is about 153 meV and Bohr radius of the exciton is given by $a_B=\frac{2\pi\varepsilon_0}{E_b} \approx 7$ Å.

Because of the unidirectional confinement in the IQW, the exciton is discretized in this direction (z direction). So the symmetry group O_h is reduced to D_{4h}. As a result, the threefold degenerate ortho-exciton $^3\Gamma_5^+$ is split into twofold degenerate $^2\Gamma_5^+$ and nondegenerate $^1\Gamma_4^+$ ortho-exciton levels, which we are going to refer to as "heavy hole exciton" and "light hole exciton" in analogy with the well known case of dipole allowed exciton. Another remarkable result of the confinement is that the para-exciton $^1\Gamma_2^+$ changes its symmetry to $^1\Gamma_3^+$. Due to the fact that the quadrupole operator $^3\Gamma_5^+$ also reduces its symmetry to $^2\Gamma_5^+$ and $^1\Gamma_3^+$, the para exciton is no longer forbidden in the IQW. Note that roughness of the interface due to the small width of the IQW leads to further reduction of the symmetry to D_{2h}. The details of the selection rules and dependence upon polarization can be found in Tables I and II.

Now, let us consider the effect of confinement on the energy spectrum of the quadrupole active exciton. We study only the ortho exciton (the generalization to the case of para exciton is trivial) and neglect spin-dependent exchange interaction and related spin-orbit effects. The energy of the $1S$ quadrupole exciton confined in a IQW can be written as

$$H_{WE} = H_e(z_e) + H_h(z_h) + \frac{p^2}{2\mu} + \frac{P^2}{2M} - \frac{e^2}{\varepsilon\sqrt{\rho^2+(z_e-z_h)^2}},$$

where ρ is the relative electron e-hole h position, p is the relative momentum, and P is the center of mass quasimomentum which is to be considered in the x, y plane. μ and M are the reduced mass and total mass of the exciton, respectively.

The quadrupole exciton confined in the infinite IQW has a smaller Bohr radius than in the case of bulk and as a result, one must take into account so-called central cell corrections[11] (CCCs) in determining the dispersion (see Fig. 2).

Aside from the nonparabolicity of the bands,[12] the electron-hole interaction in this case is the bare Coulomb interaction modified by the $\mathbf{k}$ dependent dielectric function.

TABLE II. Selection rules for the exciton in a Cu_2O quantum well. F, forbidden transition; A, allowed transition.

		D_{4h}						
		Electric dipole operator		Electric quadrupole operator				
Symmetry		$^1\Gamma_2^-$	$^2\Gamma_5^-$	$^2\Gamma_5^+$	$^1\Gamma_3^+$	$^1\Gamma_4^+$	$^1\Gamma_1^+$	Basis
Para exciton	$^1\Gamma_3^+$	F	F	F	F	F	A	(x^2-y^2)
Ortho exciton	$^1\Gamma_4^+$	F	F	F	F	A	F	xy
	$^2\Gamma_5^+$	F	F	A	F	F	F	$yz;zx$
Basis		$z;x$	z	$yz;zx$	x^2-y^2	xy	R	

This is mainly due to virtual LO-phonon assisted valence electron transition into the highest conduction bands ($^4\Gamma_8^-$ split by the confinement). Here, we have to assume that the energy of the LO-phonon modes exceeds 87 meV,[13] when the dielectric constant drops from $\varepsilon_0=7.5\mp0.2$ to $\varepsilon_\infty=6.46$. In this case, it can be shown[11] that for small values of the exciton wave number k, $\varepsilon(k)\approx\varepsilon_\infty-0.18(ka)^2$.

In our model, due to the comparable sizes of the exciton radius and IQW width, one can consider the confinement as a small perturbation to the pure 2D exciton energy. To explicitly show the perturbation part, it is convenient to introduce a small variational parameter λ ranging from 1 for pure 2D to 1/2 for pure bulk cases, so that the confined exciton energy can be rewritten as

$$H_{WE}=H_{WE}^0+H_{WE}^1+H_{WE}^2, \tag{1}$$

where we separate the analytically solvable part:

$$H_{WE}^0=H_e(z_e)+H_h(z_h)+\frac{p^2}{2\mu}+\frac{P^2}{2M}-\frac{\lambda e^2}{\varepsilon\rho}, \tag{2}$$

and small perturbation parts are due to the weak confinement:

$$H_{WE}^1=\frac{\lambda e^2}{\varepsilon\rho}-\frac{e^2}{\varepsilon\sqrt{\rho^2+(z_e-z_h)^2}} \tag{3}$$

and

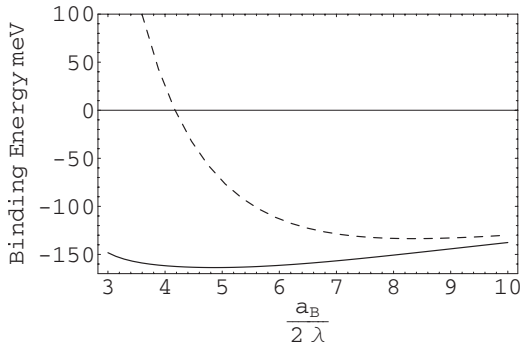

FIG. 2. The solid line shows the modified energy of the 1*S* exciton as a function of the Bohr radius (Å) and variational parameter λ due to the confinement effect; the dotted line shows the same function with the central cell correction not taken into account.

$$H_{WE}^2=\frac{p^4a^2}{24\hbar^2\mu'}-\frac{p^2P^2a^2}{4\hbar^2M'}. \tag{4}$$

These terms [Eqs. (3) and (4)] come from second order corrections in the tight-binding model and are due to nonparabolicity of the bands with $1/\mu'=C_e/m_e+C_h/m_h$ and $M'=m_e/C_e+m_h/C_h$. The second term in Eq. (4) couples the relative motion of the electron and hole with the motion of their center of mass and modifies the total exciton mass. The fourth term in Eq. (2) and second term in Eq. (4) yield the free exciton dispersion relation for the center of mass motion:[11]

$$E_{\mathbf{k}}=\frac{\hbar^2k^2}{2M}\left[1-\frac{2\lambda^2Ma^2}{M'a_B^2}\frac{I_4\left(\frac{k_Da_B}{2\lambda}\right)}{I_2\left(\frac{k_Da_B}{2\lambda}\right)}\right], \tag{5}$$

where k_D is the Debye wave vector, i.e., the radius of a sphere with volume equal to that of the first Brillouin zone and $I_n(x)=\int_0^x\frac{y^n dy}{(1+y^2)^4}$. Kavoulakis *et al.*[11] estimated the order of magnitude of the constants C_e and C_h using the $\mathbf{k}\cdot\mathbf{p}$ perturbation theory. Mixing of bands with different parities modifies the bare electron and hole masses. In addition, including the coupling to LO modes gives $C_e\approx C_h\approx1$.

In our work, we are going to use a simplified approach instead of the $\mathbf{k}\cdot\mathbf{p}$ perturbation theory and estimate this correction from the fact that the exciton is becoming localized as the Bohr radius approaches the lattice constant: $\lim_{a_B\to a} E_{\mathbf{k}}=0$. This yields the following expression: $C=2I_2(\pi)/I_4(\pi)$. The correction to the potential energy due to the first term in Eq. (4) is given by its expectation value in momentum space,

$$-\frac{\hbar^2a^2}{24\mu'}\left(\sum_{q<k_D}|\Psi_{\mathbf{q}}|^2q^4\right)\left(\sum_{q<k_D}|\Psi_{\mathbf{q}}|^2\right)^{-1}=-\frac{\hbar^2a^2C}{24\mu}\frac{I_6\left(\frac{k_Da_B}{2\lambda}\right)}{I_2\left(\frac{k_Da_B}{2\lambda}\right)}.$$

Here, the relative electron *e*-hole *h* motion wave function $\Psi_{\mathbf{q}}=\frac{8\sqrt{\pi a_B^2}}{[1+(qa_B)^2]^2}$ is strongly peaked in momentum space. The last term in H_{WE}^0 describes the effective interaction between an electron and a hole at momentum transfer q with the same

approximation for the **k** dependent dielectric function as above:

$$V(q) = \frac{4\pi e^2}{q^2 \varepsilon(q)} \approx \frac{4\pi e^2}{q^2 \varepsilon_\infty} + \frac{4\pi e^2}{\varepsilon_\infty} a^2 0.18.$$

If one truncates the $1S$ trial wave function outside the first Brillouin zone, we find the correction due to the small Bohr radius of the exciton in the form

$$-\frac{0.36\lambda^3 e^2 a^2}{\pi \varepsilon_\infty^2 a_B^3} \frac{\left[I_2'\left(\frac{k_D a_B}{2\lambda}\right)\right]^2}{I_2\left(\frac{k_D a_B}{2\lambda}\right)}.$$

In the above expression, the contribution of LO phonons to the dielectric function has been employed, where the main contribution comes from virtual transitions between the higher Γ_8^- conduction band and the highest Γ_7^+ valence band. Now, treating H_{WE}^1 as perturbation in the lowest order [neglecting momentum dependence of the screening and approximating $H_e(z_e)+H_h(z_h)+\frac{P^2}{2M}$ by $\frac{\hbar^2\lambda^2}{\mu a_B^2}$], one can find the total Wannier-Mott exciton energy in the IQW as the minimum of the total exciton energy with respect to the Bohr radius:

$$E_{WE}^{total}(\lambda, a_B) = \frac{\hbar^2\lambda^2}{\mu a_B^2} - \frac{2\lambda e^2}{\varepsilon_\infty a_B} - \frac{\hbar^2 a^2 C}{24\mu} \frac{I_6\left(\frac{k_D a_B}{2\lambda}\right)}{I_2\left(\frac{k_D a_B}{2\lambda}\right)} - \frac{0.36\lambda^3 e^2 a^2}{\pi \varepsilon_\infty^2 a_B^3} \frac{\left[I_2'\left(\frac{k_D a_B}{2\lambda}\right)\right]^2}{I_2\left(\frac{k_D a_B}{2\lambda}\right)}. \quad (6)$$

To find the variational parameter λ, we use an additional restriction determined by requiring that the first order energy shift vanishes:[14]

$$\langle \Psi_\lambda | H_{WE}^1 | \Psi_\lambda \rangle = 0, \quad (7)$$

$$\Psi_\lambda = \chi_e(z)\chi_h(z) \frac{(2\lambda)^{3/2} \exp\left(-\frac{2\lambda\rho}{a_B}\right)}{\sqrt{\pi a_B^3}} e^{-i\mathbf{k}\mathbf{r}_\parallel}, \quad (8)$$

where Ψ_λ is the unperturbed eigenfunction of H_{WE}^0. The envelope functions for the confined electron and hole are denoted as χ_e and χ_h correspondingly and that for $k=0$ is given by Eq. (14). The numerical calculations (see Figs. 2 and 3) show that for a monolayer of the cuprous oxide, $\lambda \approx 0.881$, $a_B \approx a = 4.6$ Å, i.e., in this case, one can consider the $1S$ quadrupole exciton to be Frenkel-like localized exciton with k dependent oscillator strength.

Without central cell corrections, the value of the binding energy is 124 meV (minimum of the dashed curve on Fig. 2). With CCC, it lowers to 154 meV and it corresponds to the minimum on the lower solid curve of Fig. 2. Now, in the weak confinement of the IQW, there is a restriction on the value of the parameter λ given by Eq. (7). So the standard binding energy (second term in the total energy [Eq. (6)] slightly grows with the increasing parameter λ.[15] But the CCC with increasing confinement λ decreases. This results in bigger binding energy for weak confinement than that for the bulk case without CCC but slightly smaller than that for the bulk case with CCC. This unusual behavior is entirely attributed to the confinement dependent CCC.

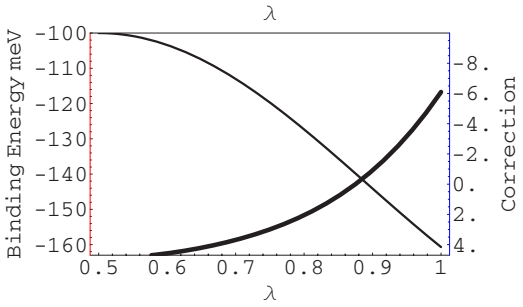

FIG. 3. (Color online) For numerical estimation of the confined quadrupole Bohr radius as an approximation, we took a_B to be the bulk Bohr radius of 5.1 Å. So the "correction" equation [Eq. (7)] becomes a function of only one parameter λ, and so does the binding energy [Eq. (6)].

The confinement in the IQW increases the overlap of the electron and hole wave functions, which, in turn, increases the oscillator strength of the yellow transition. We are only able to estimate the oscillator strength in the case of quantum confinement. We consider a non radiative interface exciton, which refers to the states outside the photon cone, $k \geqslant \frac{\omega\sqrt{\varepsilon}}{\hbar c}$. The exciton propagating in the plane is trapped and accompanied by the light field which is evanescent in the direction perpendicular to the interface (if one considers formation of polariton modes), i.e., invisible at macroscopic distances from the IQW. In the strictly two-dimensional limit, the oscillator strength of the lowest state scales as $\frac{f^{2D}}{Sa_B} \sim (\lambda_k)^{-3}/a_B^3$. The oscillator strength per unit volume scales as $\frac{f^{3D}}{V} \sim \frac{1}{a_B^3}$. The maximum enhancement of the oscillator strength in IQW with respect to the bulk case is eight times and results in giving $f^{2D} \approx 8(3.7\times 10^{-9})$. In general, due to the interaction with the Frenkel exciton, f^{2D} will have weak dependence on the wave vector. Also, the exciton resonance broadens due to imperfections of the IQW. In our case, the IQW is rather thin, which gives rise to interface roughness and thickness fluctuations. Therefore, the exciton mode should show a linewidth of about 1 μeV (lifetime ≈1.7 ns).

IV. PS:CA:DCM2 AS AN ORGANIC PART OF THE HYBRID

As it was already discussed, for the best manifestation of the hybridization effect, one has to be able to tune the energy of the Frenkel and Wannier-Mott excitons into resonance. Also, the Frenkel exciton lifetime should be comparable to the lifetime of the $1S$ quadrupole exciton, otherwise the hybrid would not live long enough to utilize, the peculiar properties of the quadrupole part. So we decided to use in our

model the Frenkel exciton formed in a recently reported amorphous organic thin film doped with the red laser dye, DCM2,[16] which has an electric dipole moment $d_x^F \approx 11$ D in the ground state. To achieve a red spectral shift of DCM2 into resonance with the 1*S* quadrupole exciton, we propose to use a low DCM2 dopant concentration in a two component host consisting of PS and the polar small molecule CA.

Because DCM2 and CA (dipole moment ≈6 D) are highly polar molecules and PS is a nearly nonpolar (less than 1 D), one can adjust the spectral shift by means of adjusting the relative concentration of the DCM2 and CA molecules. Increasing the DCM2 concentration increases the strength of the local electric fields present in the film. In our case, we will keep DCM2 concentration constant and low (0.05%), to avoid overlapping of the organic and inorganic excitons and limiting of DCM2 aggregation effects. At the same time, the dielectric properties of the film are modified by changing the concentration of CA, which has a large ground state dipole moment relative to its molecular weight and is optically inactive in the relevant region of the DCM2 photoluminescence. The dielectric permittivity increases with increasing CA concentration linearly:

$$\tilde{\epsilon} = 2.44 + 0.13(\text{CA \%}). \tag{9}$$

In contrast, the index of refraction $n \approx 1.55$ of the film is nearly constant. The PS provides a transparent, nonpolar host matrix. Such a mechanism for the spectral shift was termed solid state solvation, the solvation mechanism underlying "solvatochromism" of organic molecules in liquids.[17]

The theory of solvatochromism relates the experimentally observed changes in emission and absorption spectra of a solute (DCM2) to the dielectric permittivity of a solvent (PS:CA). An electronic transition on the solute (due to photon absorption) produces a corresponding change in the solute charge distribution, which causes the surrounding solvent molecules to respond to this new field apart from the Frank-Condon (FC) shift due to solute nuclear reorganization (see Fig. 4 for details) in two ways:

(1) The first is through electronic cloud reorganization (polarizability) which is referred to as "fast" solvation which occurs for 0.16 fs judging from the relaxation spectrum of the DCM2 (linewidth ≈0.25 eV).

(2) The second is through gross spatial movement due to physical translation and rotation ("slow" solvation). During this phase, the radiative recombination from the FE is prohibited and allows the FE exciton to live for 3.3 ns. In our proposed scheme, the actual hybridization with 1*S* quadrupole exciton occurs during this time interval as it is comparable to the lifetime of the quantum confined quadrupole exciton, while the lifetime of the DCM2 in vacuum is determined by the FC effect which is much faster.

Once the Frenkel exciton energy falls into the nonzero coupling parameter vicinity with the quadrupole exciton (resonance condition), the hybridization occurs. The detailed dynamics of the hybrid is the subject of our future work. Presently, we assume that the effective lifetime of the hybrid is $\frac{\tau_s \tau_{1S}}{\tau_s + \tau_{1S}}$ and requires two photons to populate both branches of the hybrid exciton. We performed calculations for the energy of the Frenkel exciton under the "continuum" approximation, in which the surrounding molecules of the solvent are replaced by a continuous dielectric. The molecules of the solute are described by a spherical cavity of radius a_F of the DCM2 molecules and corresponding charge distribution is reduced to the dominant dipole moment.[18] Then, the total emission energy including solvation effect can be written as

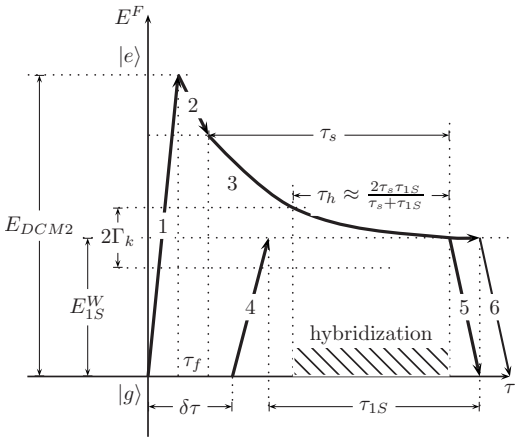

FIG. 4. Schematic of dynamic tuning of Frenkel and 1*S* quadrupole Wannier excitons by means of solid state solvation redshift effect. Following (1) photon absorption in DCM2, there are distinct dynamic phases: (2) fast adjustment of the electronic configuration in DCM2 due to interaction with polar CA molecules within the time frame of picoseconds, τ_f; (3) slow self-adjustment of DCM2 and CA molecules with $\tau_s \approx 3.3$ ns; (4) absorption of second yellow photon delayed by $\delta\tau \approx \tau_s - \tau_{1S}$ by Cu_2O confined 1*S* quadrupole exciton with lifetime $\tau_{1S} \approx 1.7$ ns; hybridization when detuning between this two types of exciton becomes smaller than the *k* dependent coupling parameter; lifetimes of the hybrid are defined by τ_s and τ_{1S}; (5) phosphorescence due to the hybrid exciton recombination. (6) shows possible recombination of noninteracting excitons.

$$E = E_0 + \Delta E_{solv}, \tag{10}$$

where E_0 is the emission energy in vacuum including the FC shift, and $E_{solv} = -\frac{1}{a_F^3}(\mu_g - \mu_e)(\Lambda\mu_e + \Lambda_{op}\mu_g)$; here, we introduced μ_e and μ_g to be, respectively, solute excited and ground state dipoles and

$$\Lambda = \frac{2(\tilde{\epsilon} - 1)}{2\tilde{\epsilon} + 1}, \quad \Lambda_{op} = \frac{2(n^2 - 1)}{2n^2 + 1}$$

associated with slow and fast relaxation processes (described above), respectively.

Equations (9) and (10), along with experimental fitting for $-\frac{1}{a_F^3}(\mu_g - \mu_e)\mu_e = 0.57$, yield the concentration of the CA ≈22% to correspond to the resonance with the confined 1*S* quadrupole energy of 2.05 eV.

There is one sensitive point we make in our work, namely, necessity of the second delayed photon. One photon does allow hybridization once the energy of the FE is close enough. Only one branch of the hybrid is going to be populated. Because we approach the resonant energy from above, the upper branch is the one to be populated. The lower branch may be populated by a multiacoustical phonon pro-

cess. However, first, we do not know how long it takes to populate from the maximum of the upper branch to the minimum of the lower branch. For the temperature of 1.7 K, it takes approximately 26 of such phonon processes without the Stark effect (see Sec. V) or 7 of them with the Stark effect. Even though such transitions are allowed, it may take more time than the lifetime of the hybrid. For example, the lifetime of the $1S$ orthoexciton itself is determined by the acoustical phonon assisted transformation to the paraexciton, which involves change in energy of 12 meV, which is comparable to $2\Gamma_k$.

So the second photon is designed to assure that both branches are populated regardless of the initial conditions. When both photons are in resonance with the WE, $\hbar\omega \approx E_{1S}$, the second photon provides conservation of the energy:

$$\hbar\omega + \hbar\omega = (E_{1S} + \Gamma_k) + (E_{1S} - \Gamma_k).$$

V. INDUCED STARK EFFECT

In this section, we investigate a new effect which plays a rather significant role in forming any hybrid exciton. Let us refer to it as an induced quantum confined Stark effect. The main idea is as follows. There is an evanescent potential in the z direction and corresponding $\mathbf{k}$ dependent electric field due to the Frenkel organic (DCM2) exciton, penetrating into the inorganic quantum well (see Fig. 1). This field induces some polarization of the bound electron-hole pairs forming the Wannier-Mott inorganic exciton. This polarization leads to an effective screening of the electric field and results in reducing the coupling.

We consider the FE as polarization wave[2] $\mathbf{P}(\mathbf{r})$ confined to a perfectly 2D organic quantum well placed at position $z' \approx \frac{L_w}{2}$. Neglecting the constant phase of the wave $e^{-i\frac{\mathbf{k}\mathbf{L}_w}{2}}$, the polarization per unit area S is given as

$$\mathbf{P}(\mathbf{r}) = a_F \mathbf{d}^F \frac{e^{-i\mathbf{k}\mathbf{n}_\parallel}}{\sqrt{S}} \delta\left(z - \frac{L_w}{2}\right).$$

Now let us move from the discrete set of FE to a continuous distribution and take into account that

$$\sum_{\mathbf{n}} e^{-i\mathbf{k}\mathbf{n}_\parallel} = \frac{1}{a_F^2} \int e^{-i\mathbf{k}\mathbf{r}_\parallel} d\mathbf{r}_\parallel.$$

In this continuous approximation, one gets the final result for the polarization created by the FE propagation along the interface:

$$\mathbf{P}(\mathbf{r}) = \mathbf{d}^F \frac{e^{-i\mathbf{k}\mathbf{r}_\parallel}}{a_F\sqrt{S}} \delta\left(z - \frac{L_w}{2}\right) + \text{c.c.}$$

The potential due to this polarization wave is given by[2]

$$\varphi_{\mathbf{k}}(\mathbf{r}) = G(\mathbf{r}, \mathbf{n}_\parallel, \mathbf{k})\, \nabla\, \mathbf{P} = -\nabla_i G(\mathbf{r}, \mathbf{n}_\parallel, \mathbf{k}) \mathbf{P}_i.$$

The standard Green's function for $z < z'$ is given by

$$G(z, z', \mathbf{k}) = \frac{4\pi}{\varepsilon(\mathbf{k}) + \tilde{\varepsilon}} \frac{e^{k(z-z')}}{k}.$$

It gives rise to the potential of the form

$$\varphi_{\mathbf{k}}(\mathbf{r}) = \sum_i (k\delta_{i,z} + ik) G(\mathbf{k}, z', z) \mathbf{P}_i(\mathbf{r}) = \varphi_{\mathbf{k}}(\mathbf{r})$$

$$= \mathbf{d} \frac{e^{-i\mathbf{k}\mathbf{r}_\parallel}}{a_F\sqrt{S}} \frac{4\pi}{\varepsilon + \tilde{\varepsilon}} e^{k(z-z')}. \tag{11}$$

Here, we utilized the fact that the complex conjugate part cancels out the imaginary part of the above expression. The electric field creates an additional polarization in the IQW, which we are going to estimate by its effect upon the coupling parameter. Effectively, this polarization manifests itself in an envelope function equation in the IQW for the electron and hole. Following a standard procedure (Bastard[19]), the equations governing the electron (hole) envelope function in the IQW are as follows:

$$\left(-\frac{\hbar^2}{2m_e}\frac{d^2}{dz^2} - eF_{\mathbf{k}} z\right) \chi^e_{\mathbf{k}}(z) = (E - E_c) \chi^e_{\mathbf{k}}(z),$$

$$\left(-\frac{\hbar^2}{2m_h}\frac{d^2}{dz^2} + eF_{\mathbf{k}} z\right) \chi^h_{\mathbf{k}}(z) = (E_v - E) \chi^h_{\mathbf{k}}(z),$$

where we used the long wave approximation for the potential, namely, taking the effective electric field in the form $F_k \simeq k\varphi_{\mathbf{k}}(z=z')$. The total energy shift due to the induced field is negligible for small difference in the electron and hole masses and small width of the IQW. The envelope functions are subject to zero boundary conditions at both sides of the IQW. Here, one comes across some difficulties. Although this system has an exact solution, the standard approach with Airy functions Ai and Bi will lead us to a rather complicated but exact result:

$$\chi^n_k(z) = C_{1,n,k}\, \text{Ai}\left(\frac{eF_k z - \zeta_{n,k}}{\zeta_{0,k}}\right) + C_{2,n,k}\, \text{Bi}\left(\frac{eF_k z - \zeta_{n,k}}{\zeta_{0,k}}\right). \tag{12}$$

In the last expression, we introduce the following notation for the electron (hole) energy change due to the confinement and FE induced polarization:

$$\zeta_{0,k} = \left[\frac{(eF_k\hbar)^2}{2m}\right]^{1/3},$$

$$\zeta_{n,k} = E_n - E_0 - e\varphi_{\mathbf{k}}(0),$$

with $E_0 = 0$ for the electron and $E_0 = -E_g$ for the hole (we also omitted indices e and h for simplicity). The normalization constants are connected as

$$C_{1,n,k} = \frac{\mathrm{Ai}\left(\dfrac{eF_k\dfrac{L_w}{2} - \zeta_{n,k}}{\zeta_{0,k}}\right)}{\mathrm{Bi}\left(\dfrac{eF_k\dfrac{L_w}{2} - \zeta_{n,k}}{\zeta_{0,k}}\right)}.$$

The energy levels can be found using boundary conditions as discrete solutions for

$$\mathrm{Ai}\left(\frac{eF_k\frac{L_w}{2} - \zeta_{n,k}}{\zeta_{0,k}}\right)\mathrm{Bi}\left(\frac{-\zeta_{n,k} - eF_k\frac{L_w}{2}}{\zeta_{0,k}}\right) - \mathrm{Bi}\left(\frac{eF_k\frac{L_w}{2} - \zeta_{n,k}}{\zeta_{0,k}}\right)\mathrm{Ai}\left(\frac{-\zeta_{n,k} - eF_k\frac{L_w}{2}}{\zeta_{0,k}}\right) = 0. \quad (13)$$

The constant is defined from the normalization condition. For the hole, one has to change $e \to -e$. Although Eqs. (13) and (12) exhibit the exact solution, they are rather complicated for further analytical description of the hybrid exciton states.

There are some approximate ways to treat the problem of relative shift of the electron and hole wave functions in the induced field. First, let us treat the electric field F_k using the perturbation theory. In this approach, we can explicitly see the term due to the induced polarization. This perturbation approach is applicable if the energy difference between the unperturbed ground and first exited states is much bigger than the perturbing potential at the average position of the particle $z=0$. For the case of a monolayer of Cu_2O, it is applicable only for the very small wave vector region but may be used as a correction in the dipole-dipole hybridization. In the first order, there will be no change in total energy ($\propto F_k^2$), but the wave functions will be changed to

$$\chi_k^e(z) = \sqrt{\frac{2}{L_w}}\cos\left(\frac{\pi z}{L_w}\right) - \frac{32F_kL_w^3em}{27\pi^2\hbar^2}\sqrt{\frac{1}{L_w}}\sin\left(\frac{2\pi z}{L_w}\right). \quad (14)$$

Because Eq. (14) is still rather complicated, we will consider only the lowest energy level transitions, so it is possible to consider (instead of the infinite IQW) an "equivalent" parabolic profile defined through its lowest energy level as

$$\frac{1}{2}\hbar\omega_0^2 = \frac{(\pi\hbar)^2}{2mL_w}.$$

So we are able to consider $\mathbf{k}$ and L_w values in the region where the perturbation theory is not applicable. This problem has the exact solution with the same energy as was given by the perturbation theory for the lowest transition. The envelope function normalized inside the given IQW has a Gaussian form:

$$\chi_{\mathbf{k}}^{e,h}(z) = \frac{(2\pi)^{1/4}}{\sqrt{\mathrm{erf}(\pi\sqrt{2})L_w}}\exp\left[-\frac{(z-z_{e,h})^2}{R_0^2}\right]. \quad (15)$$

In Eq. (15), the dimension R_0 of the parabolic IQW for the electrons and holes is taken to be the same:

$$R_0 = \sqrt{\frac{\hbar}{m_e\omega_0}} = \frac{L_w}{\pi}.$$

The shifted average electron and hole positions are given by

$$z_{e,h} = \pm\frac{eF_k^2}{2m\omega_0^2} = \pm\frac{eF_k^2mL_w^4}{2\pi^4\hbar^2}.$$

In the next section, we are going to use these results for the envelope function to calculate the coupling parameter.

VI. THE COUPLING PARAMETER AND DISPERSION

The energy of interaction between the organic dipole and inorganic $1S$ quadrupolar excitons can be written as[20]

$$\hat{H}_{int} = -\frac{1}{6}\sum_{\alpha}\sum_{\beta}\hat{Q}_{\alpha\beta}\frac{\partial}{\partial x_\alpha}\hat{F}_\beta = -\frac{1}{6}\hat{Q}_{\alpha,\beta}|0\rangle D_{i,\alpha,\beta}(\mathbf{n}-\mathbf{r}_\parallel, z', z) \times\langle 0|\hat{d}_i^F,$$

where $\hat{Q}_{\alpha\beta}$ is a quadrupole transition operator; the electric field operator $\hat{F}_\beta$ is due to the Frenkel exciton as in Eq. (11); $D_{i,\alpha,\beta}$ is the Green's function in momentum space. The interaction parameter is given by the following transition matrix element:

$$\Gamma_{\mathbf{k}} = \langle W,\mathbf{k}|H_{int}|F,\mathbf{k}\rangle = \sum_{\alpha,\beta,i}\sum_{\mathbf{n}}\int dz d\mathbf{r}_\parallel\langle W,\mathbf{k}|\hat{H}_{int}|F,\mathbf{k}\rangle.$$

The quadrupole transition matrix element may be obtained by using the relation $\frac{1}{S}\Sigma_{\mathbf{q}}\varphi_{1S}(\mathbf{q}) = \varphi_{1S}(\mathbf{r}_e - \mathbf{r}_h = 0)$ between the wave function of the relative electron-hole motion of the $1S$ exciton φ_{1S} normalized to the unit area S and its momentum representation $\varphi_{1S,\mathbf{q}}$. Hence, the Fourier component of the quadrupole exciton transition from the ground state of the crystal[21] is given as

$$\langle W,\mathbf{k}|\hat{Q}_{\alpha,\beta}|0\rangle = \frac{e^{i\mathbf{k}\mathbf{r}_\parallel}}{\sqrt{S}}\sum_{\mathbf{q}}\varphi_{1S}(\mathbf{q})Q_{\alpha,\beta}(\mathbf{q}) = \sqrt{\frac{2}{\pi}}\frac{\lambda Q_{\alpha,\beta}}{a_B}\frac{e^{i\mathbf{k}\mathbf{r}_\parallel}}{\sqrt{S}}\chi_k^e(z)\chi_k^h(z).$$

Considering the weak dependence of the conduction $u_{c,q}$ and valence $u_{v,q}$ Bloch functions on the wave vector $\mathbf{q}$, the quadrupole moment of the interband transition may be written as

$$Q_{\alpha,\beta} \approx Q_{\alpha,\beta}(\mathbf{q}=\mathbf{0}) = \frac{1}{v_0}\int_{v_0} d\mathbf{s}u_{c\mathbf{q}}^*(\mathbf{s})x_\alpha x_\beta u_{v\mathbf{q}}(\mathbf{s}),$$

with the integration taken over the unit cell of the cuprous oxide v_0. The expectation value of the FE dipole transition operator is given as

TABLE III. Green's function selection rules.

	Q_{xy}	Q_{xz}	Q_{yz}
$\mathbf{k}_{[1,0,0]}$	$D_{xxy}=0$	$D_{xxz}=-\frac{4\pi}{\varepsilon+\tilde{\varepsilon}}k^2e^{k(z-z')}$, $\mathbf{d}=(d_x,0,0)$	$D_{xyz}=0$
	$D_{yxy}=0$	$D_{yxz}=0$	$D_{yyz}=0$
	$D_{zxy}=0$	$D_{zxz}=i\frac{4\pi}{\varepsilon+\tilde{\varepsilon}}k^2e^{k(z-z')}$, $\mathbf{d}=(0,0,d_z)$	$D_{zyz}=0$
$\mathbf{k}_{[0,1,0]}$	$D_{xxy}=0$	$D_{xxz}=0$	$D_{xyz}=0$
	$D_{yxy}=0$	$D_{yxz}=0$	$D_{yyz}=-\frac{4\pi}{\varepsilon+\tilde{\varepsilon}}k^2e^{k(z-z')}$, $\mathbf{d}=(0,d_y,0)$
	$D_{zxy}=0$	$D_{zxz}=0$	$D_{zyz}=i\frac{4\pi}{\varepsilon+\tilde{\varepsilon}}k^2e^{k(z-z')}$, $\mathbf{d}=(0,0,d_z)$
$\mathbf{k}_{[0,0,1]}$	$D_{xxy}=0$	$D_{xxz}=0$	$D_{xyz}=0$
	$D_{yxy}=0$	$D_{yxz}=0$	$D_{yyz}=0$
	$D_{zxy}=0$	$D_{zxz}=0$	$D_{zyz}=0$

$$\langle 0|\hat{d}_i^F(\mathbf{n})|F,\mathbf{k}\rangle = \sqrt{\frac{\pi}{S}}a_F d_i^F e^{-i\mathbf{kn}}.$$

The Green's function in momentum space for the given geometry is given by

$$D_{i,\alpha,\beta}(\mathbf{k},z',z) = \frac{4\pi}{\varepsilon+\tilde{\varepsilon}}k^2e^{k(z-z')}\left(\frac{ik_i}{k}+\delta_{i,z}\right)\left(\frac{ik_\beta}{k}+\delta_{\beta,z}\right)\left(\frac{ik_\alpha}{k}+\delta_{\alpha,z}\right).$$

For the selection rules based on the specific geometry of the problem and the corresponding Green's function, see Table III. Without loss of generality, we may take the wave vector along the x axis. From the Green's function, polarization selection rules,[22] our specific type of interaction energy, and the requirement of having real eigenvalues, one can conclude that the only possible direction of the wave vector and dipole orientation is d_x^F and $Q_{x,z}$ respectively.

We note here that there is another possible approach to the problem of resonant interaction between these two types of exciton. If one modifies the results of Moskalenko and Liberman[21] for our case and introduce an effective polarization due to quadrupole transitions via a $\mathbf{k}$ dependent interband dipole element,

$$\mathbf{d}_{ij,\mathbf{k}} \sim |Q_{ij}|(\mathbf{e}_i k_j + \mathbf{e}_j k_i), \tag{16}$$

then one uses the corresponding interband polarization, this would coincide with a case of "dipole-dipole" transitions, when the electric field created by the set of WE dipoles will interact with the dipoles in the organic. In this way, one could directly use the results of Agranovich *et al.*[1] Due to an additional requirement for the Hamiltonian to be Hermitian, it would give us the following result for the coupling constant:

$$\Gamma_{i\neq j}(\mathbf{k}) \sim \mathrm{Re}(\mathbf{d}_{ij,\mathbf{k}}^W D_{j\alpha}\mathbf{d}_\alpha^F) \sim |Q_{x,j}|d_x^F k_x \mathbf{e}_j\mathbf{e}_x.$$

Here we used the fact that the wave vector has only an x component. So this coupling parameter vanishes in this approximation as $j\neq x$. For that reason, in this article, we study the interaction of the cuprous oxide quadrupole with the gradient of the electric field created by the organic Frenkel exciton placed near the interface between the organic PS:CA and inorganic Cu_2O.

Calculating the integral of the coupling parameter and summing over the dipoles for the case when a perturbation approach is applicable yields

$$\Gamma(\mathbf{k}) = \Gamma_1(\mathbf{k}) + \Gamma_2(\mathbf{k}).$$

Here $\Gamma_1(\mathbf{k})$ corresponds to the unperturbed coupling parameter, and the last term is due to the perturbation,

$$\Gamma_1(\mathbf{k}) = \frac{8\sqrt{2\pi}}{6[\varepsilon(k)+\tilde{\varepsilon}]L_w}\frac{ke^{-kz'}\sinh\left(\frac{L_w k}{2}\right)}{\left[1+\left(\frac{kL_w}{2\pi}\right)^2\right]}\frac{Q_{xz}d_z^F}{a_F a_B L_w}. \tag{17}$$

To increase this coupling term, one may consider the organic host PS:CA with DCM2 organized in a multilayered structure. Generalizing the same approach to this case of multilayered organic with distance between the layers equal to twice the radius of the Frenkel exciton (compact composition), it can be shown that one has to multiply Eq. (17) by $\left(\frac{2\cdot e^{2ka_F}}{e^{2ka_F}-1}\right)$. The factor of 2 in the last expression indicates that the organic is placed on both sides of our IQW and one must consider the symmetrical Green's function in the interaction.

Another term in the coupling parameter is due to the induced Stark effect[23] and has the form

$$\Gamma_2(\mathbf{k}) \sim -\frac{512}{27}\frac{L_w^4 k F_\mathbf{k} CM}{\pi^2\hbar^2}\frac{e\cosh\left(\frac{kL_w}{2}\right)}{k^4L_w^4+10\pi^2k^2L_w^2+9\pi^4},$$

where $F_\mathbf{k}$ is the electric field induced by the organic layer of dipoles and the terms proportional to L_w^6 have been omitted.

For the region of wave vector and width of the IQW where one cannot use the perturbation theory, another form of the coupling parameter can be introduced. In this case, it

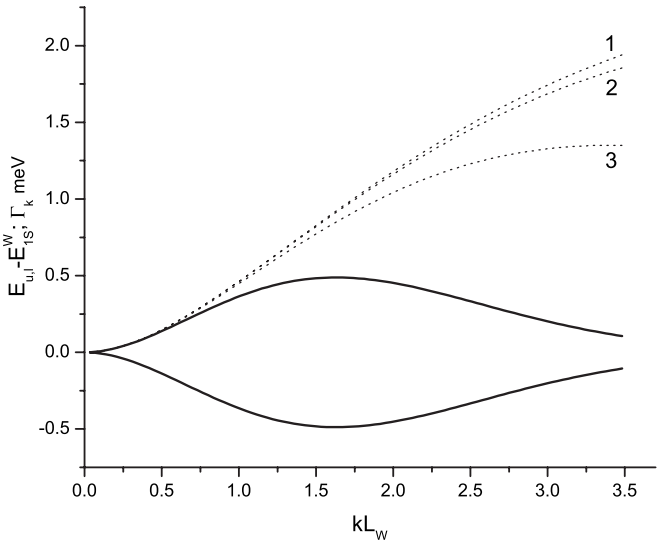

FIG. 5. The solid lines represent the upper and lower branches of the quadrupole-dipole hybrid dispersion when the coupling is calculated in the parabolic approximation and the induced Stark effect is taken into account; the dash lines correspond to the coupling parameter for different approximations: (1) infinite IQW and the induced Stark effect is neglected; (2) parabolic approximation; (3) infinite IQW with the induced Stark effect treated as a perturbation.

is convenient to use the effective parabolic potential and the envelope functions in the form of Eq. (15), and the coupling parameter has the form

$$\Gamma(k) \sim k^2 e^{-kz'} \frac{\sqrt{2}}{4} \exp\left(-\frac{16z_e^2 - R_0^4 k^2}{8R_0^2}\right)\left\{\operatorname{erf}\left[\frac{\sqrt{2}}{4}(2\pi + kR_0)\right] + \operatorname{erf}\left[\frac{\sqrt{2}}{4}(2\pi - kR_0)\right]\right\}. \quad (18)$$

Here, for simplicity, we set $z_e \approx -z_h$, or in other words, $m_e \approx m_h$. For numerical estimation of the quadrupole matrix elements, we used the well known[21] result for the corresponding oscillator strength:

$$f_{xz,\mathbf{k}_0} = \frac{4\pi m_0 E_g}{3e^2\hbar^2}\left(\frac{a_B}{2\lambda a}\right)^3 \mathbf{e}_z \mathbf{k}_{0,x} Q_{x,z},$$

where λ represents the effect of quantum confinement and $|\mathbf{k}_0| = 2.62 \times 10^5$ cm^{-1}.

The dispersion of the hybrid state in the case of negligibly small detuning of 1*S* exciton with the DCM2 transitions (resonance) is presented in Fig. 5. The first dashed lines (1) correspond to the coupling parameter when the Stark effect is neglected. So it corresponds to the upper part of the dispersion in this approximation. To show the effect of the "parabolic" approximation on the coupling, we drew the second dashed line (2). The third dashed line is when the Stark effect is small enough to be taken as a perturbation without applying the parabolic approximation.

Note that we consider the quadrupole-dipole interaction only between Cu_2O and DCM2 excitons and neglect the coupling with PS:CA host transitions, as the corresponding interband dipole moments for the transitions off-resonance with the inorganic have much smaller oscillator strength. By neglecting the Stark effect from this numerical estimation, it is easy to see that for the values of $kR_0 \ll 1$, expressions (18) and (17) are equivalent.

VII. RESULTS AND DISCUSSION

Although the oscillator strength of the 1*S* quadrupole exciton is 3 orders of magnitude smaller than that for the nearest dipole allowed exciton, strong spatial dispersion[24] makes the maximum of the coupling parameter comparable with those for the dipole-dipole case.

The 1*S* quadrupole exciton has a rather big mass ($\approx 3m_0$) and so is comparable to the mass of the Frenkel exciton ($\geqslant 5m_0$). Also, one has to take into account a significant effect of the IQW width fluctuation. Indeed, the effect of the width fluctuation is energy change between the confined and bulk cases, which corresponds to energy drop of $E_{1S,binding}(\lambda=1) - E_{1S,binding}(\lambda=0.881) = 17$ meV (see Fig. 3). Hence, due to both of these effects, we neglected the kinetic energy of the confined quadrupole 1*S* exciton (the motion occurs in Frenkel-like way, by hopping between sites of localization). Thus, the quadrupole-dipole hybridization effect is more pronounced than that of the dipole-dipole hybridization because it is not masked by the kinetic energy of the exciton.

Also, the hybridization effect is not masked by the large radiative decay rate of the Frenkel exciton. Instead of the classical spontaneous radiative rate of the organic, we use the solid state solvation process to obtain a different relaxation mechanism. Namely, one has the dynamical redshift of the DCM2 Frenkel exciton during the slow phase of the solvation process, when the energy of the photon excited DCM2 molecules is partially transferred to the polar CA molecules by nonradiative dipole-dipole electromagnetic interaction followed by immediate (compared to the τ_S) radiative decay. To compare the radiative decay rate (lifetime) with the hybridization parameter, we simplify the dynamics to the following statement. The Frenkel exciton has fixed resonant energy with the 1*S* quadrupole Wannier exciton but has effective lifetime equal to τ_S.[25] So if one omits all the possible nonradiative channels of decoherence except the radiative decay, then the radiative decay rate from the hybrid to the ground state is calculated using Fermi's golden rule:

$$\hbar\gamma_{hybrid}(u,l;k) = 2\pi|\langle g|H_{\text{int}}|u,l;k\rangle|^2\delta(\hbar\omega_k - E_{u,l}) = \frac{A_{l,u}^2\hbar}{\tau_s} + \frac{B_{l,u}^2\hbar}{\tau_{1S}} = \frac{\hbar}{2}\frac{\tau_s + \tau_{1S}}{\tau_s\tau_{1S}} \approx 0.29\ \mu\text{eV}.$$

From this estimation, the ratio of the hybrid radiative rate to the maximum of the coupling parameter is 0.0006, which is 2 orders of magnitude smaller than the predicted[2] value of 0.09 for the dipole-dipole hybrid in a quantum dot.[26] Indeed, it was shown in, the case of fully localized quantum dot dipole-dipole hybridization that the ratio of the hybrid exci-

ton damping parameter to the coupling is proportional to $\frac{i\hbar\gamma_{hybrid}}{\Gamma_k} \propto \sqrt{a_B^3}$ ($\sqrt{a_B}$ in the case of quantum wires[1]) so quadrupole-dipole hybridization takes advantage of the small radius of the 1*S* quadrupole. Also, the fact of the comparable lifetimes of the organic and 1*S* quadrupole excitons significantly influences the ratio.

A noteworthy feature of the resulting upper (u) and lower (l) branch dispersion in Fig. 5 is that the well pronounced minimum on the lower branch can be populated by pump-probe experiment and now it may be possible to have a finite critical temperature in the case of quasi-2D excitons, due to the fact of nonparabolic dispersion of the lower branch of the hybrid. This can provide a good basis for searching for BEC in such a hybrid. A new type of an interface polariton may also be expected.

Note that we mentioned the possible BEC as a possibility only. Judging from the fact of the big saturation density of the hybrid and minimum of the energy on the lower branch, this minimum would make the hybrid exciton strongly localized and many dissipative processes (such as Auger heating[27]) are going to be suppressed. Also, as we mentioned, the nonparabolic dispersion allows the system to have a finite condensation temperature contrary to the case of 2D excitons with parabolic dispersion. However, the main question about the lifetime of the hybrid is still a subject of our current research. So we do not make a concrete statement about the BEC of the hybrid but rather make an educated guess on that.

ACKNOWLEDGMENTS

We have benefited from discussion with Que Nguyen Huong. Partial support from PCS-CUNY is greatly acknowledged.

[1] V. Agranovich, D. Basko, G. L. Rocca, and F. Bassani, J. Phys.: Condens. Matter **13**, 9369 (1998).
[2] A. Engelmann, V. I. Yudson, and P. Reineker, Phys. Rev. B **57**, 1784 (1998).
[3] N. Q. Huong and J. L. Birman, Phys. Rev. B **61**, 13131 (2000).
[4] In the point of view of Moskalenko and Liberman, one can reconsider the coupling as dipole-dipole coupling, where the inorganic dipole moment is due to the "quadrupole" transitions. We show that the corresponding reinterpolation of the formula of Agranovich *et al.* fails.
[5] F. Bassani, G. L. Rocca, D. Basko, and V. Agranovich, Fiz. Tverd. Tela (Leningrad) **41**, 778 (1999).
[6] C. Madigan and V. Bulovic, Phys. Rev. Lett. **91**, 247403 (2003).
[7] D. Frohlich, G. Dasbach, G. B. Hogersthal, M. Bayer, R. Kliebera, D. Sutera, and H. Stolzb, Solid State Commun. **134**, 139 (2005).
[8] Let us consider the smallest possible fluctuation of the IQW width, i.e., it changes from L_w to $2L_w$ and decrease of the exciton energy is approximately 20 meV, which is big compared to the rather small kinetic energy of the exciton for it has a rather big mass of free exciton.
[9] R. J. Elliott, Phys. Rev. **124**, 340 (1961).
[10] E. F. Gross and N. A. Karryev, Dokl. Akad. Nauk SSSR **84**, 261 (1952).
[11] G. M. Kavoulakis, Y. C. Chang, and G. Baym, Phys. Rev. B **55**, 7593 (1997).
[12] S. A. Moskalenko and K. Tolpigo, Zh. Eksp. Teor. Fiz. **36**, 149 (1959).
[13] H. R. Trebin, H. Z. Cummins, and J. L. Birman, Phys. Rev. B **23**, 597 (1981).
[14] S. Jaziri, Solid State Commun. **91**, 171 (1992).
[15] $\lambda = 1/2$ for the bulk and $\lambda = 1$ for the maximum of the confinement (strong confinement regime).
[16] V. Bulovic, R. Deshpande, and S. Forrest, Chem. Phys. Lett. **308**, 317 (1999).
[17] M. Baldo, Z. Soos, and S. Forrest, Chem. Phys. Lett. **347**, 297 (2001).
[18] L. Onsager, J. Am. Chem. Soc. **58**, 1486 (1936).
[19] G. Bastard, *Wave Mechanics Applied to Semiconductor Heterostructures* (Halsted, New York, 1988).
[20] J. Jackson, *Classical Electrodynamics* (Wiley, New York, 1975).
[21] S. A. Moskalenko and M. A. Liberman, Phys. Rev. B **65**, 064303 (2002).
[22] Y. Liu and D. Snoke, Solid State Commun. **134**, 159 (2005).
[23] There is no induced Stark effect in the multilayered case due to the corresponding symmetry of the organic.
[24] Factor of k in Eq. (17) resulted from the quadrupole nature of the 1*S* transition in the cuprous oxide.
[25] Much better results for the decay rate of the hybrid may be obtained from a solution of the kinetic equations governing the dynamics of solvation and hybridization. This is a subject for our future work and will be reported elsewhere.
[26] We have not derived the dependence of the damping on the confinement and Bohr radius of the quadrupole-dipole hybrid. So we used the work of Engelmann *et al.* (Ref. 2) on the fully confined quantum dot hybrid, and also work of Agranovich *et al.* (Ref. 1) on the less confined quantum wire dipole-dipole confinement. This complies with our strategy to make comparative analysis between quadrupole-dipole and dipole-dipole hybrid cases.
[27] G. M. Kavoulakis, Phys. Rev. B **65**, 035204 (2001).